SIMULTANEOUS OBSERVATION OF LEO OBJECTS

Lorenzo Mariani[(1)], Gaetano Zarcone[(1)], Leonardo Parisi[(2)], Stefania Melillo[(2)], Federico Curianò[(3)], Shariar Hadji Hossein[(1)], Fabio Santoni[(3),] Fabrizio Piergentili[(1)]

(1) Department of Mechanical and Aerospace Engineering (DIMA), University of Rome "La Sapienza"; mariani_lorenzo@hotmail.it, gaetano.zarcone@uniroma1.it, shariar.hadjihossein@gmail.com, fabrizio.piergentili@uniroma1.it

(2) Institute of Complex System (ICS), National Research Council (CNR), UOS Sapienza; leonardo.parisi@cnr.it, stefania.melillo@cnr.it

(3) Department of Astronautics, Electric and Energy Engineering (DIAEE), University of Rome "La Sapienza"; federico.curiano@uniroma1.it, fabio.santoni@uniroma1.it

ABSTRACT

In recent years the increasing of space activity led to an increase in space debris, with a consequent growing international interest in Space Surveillance and Tracking (SST). The Space Systems and Space Surveillance Laboratory (S5Lab) of the University of Rome "La Sapienza" together with the Institute of Complex System (ICS) of the Nation Research Council (CNR) undertakes research on space debris with the aim of understanding the dynamics of space debris, and therefore contributing to the preservation of the space environment. This paper is focused on bi-static data collection of Leo objects observed within the IADC campaign WG1 AI 38.2 "Attitude motion characterization of LEO upper stages using different observation techniques". Preliminary results on the determination of the position and attitude of Leo objects are presented, with particular emphasis on the experimental method.

1 INTRODUCTION

According to the definition adopted by Inter-Agency Space Debris Coordination Committee (IADC) space debris are all man-made objects including fragments and elements thereof, in Earth orbit or re-entering the atmosphere, that are non-functional. Fig. 1 shows the evolution over time of the space objects [1].

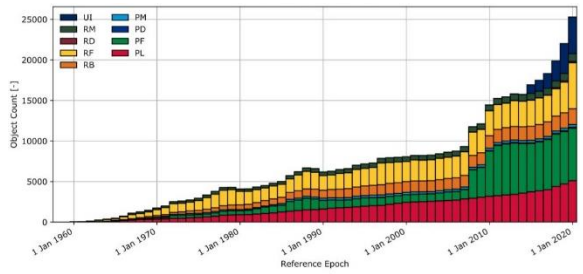

Figure 1. Evolution of space objects over the years [1]

These elements present different sizes and actually about 23'000 are tracked and catalogued [2]. Each of them represents a serious danger for operational satellites in the event of a collision [3, 4]. For the Space Situational Awareness (SSA) purposes it is necessary to monitor the behavior of the object, i.e., to model the space debris environment. In order to achieve the aim, it is possible to track the object through optical systems following its trajectory, which is known from orbital information. The only way to retrieve the orbit parameters is to use the Two-Line Elements (TLE) released by the North American Aerospace Defense Command (NORAD). Unfortunately, this set of orbital parameters is characterized by a low accuracy and short-term reliability. Therefore, frequent updates of the dynamical state estimate are necessary.

The dynamics of these objects, especially for those in the re-entry phase, is of great interest due to probability of casualties related to the ground impact of pieces surviving the atmosphere disintegration. Nevertheless, the trajectory determination of such a kind of objects is still largely affected by errors due to the difficulties in obtaining a sufficient number of measures and to the unknowns related to the atmosphere parameters and object attitude. To overcome this limitation the authors set-up a system based on bi-static optical observation, designed to collect hundreds of measures for single LEO passages from two sites simultaneously. This system has been deployed in the S5Lab observatories in Rome and Collepardo (about hundred kilometers apart) and it is operative and fully calibrated. The system permits to obtain the object accurate position thanks to the simultaneous observation, in order to increase the accuracy of trajectory determination and to obtain two light curves to be exploited for object attitude reconstruction through their inversion. This paper starts with the description of the system used to perform the bistatic optical observation (Section 2). Since the observations are simultaneous, the results of the tests useful to minimize the synchronization errors (Section 3) and the time bias analysis (Section 4) are shown. In conclusion, the results of the observation campaign both

for space debris and operative satellites are presented (Section 5).

2 BI-STATIC OPTICAL SYSTEM

To study the evolution of the behavior of an object during its orbit around the Earth, it is fundamental to know its state vector. Optical systems have proved to be an efficient method to retrieve information about orbiting bodies [5]. The research group ha several years of experience in optical observations and space systems manufacturing [6-11]. The optical systems used during this work are part of the telescope network managed by the institute research team [12], and in particular the Fast Imaging and Tracking System (FITS) was exploited. FITS is composed by telescopes located in two different places (see Fig. 2): the first one is the REmote Space Debris Observation System (RESDOS) in Rome, the latter is the Sapienza Coupled University Debris Observatory (SCUDO) in Collepardo, FR. These observatories have a mutual distance, i.e., baseline, of about 80 km. In order to avoid any kind of differences in terms of timing synchronization, obtaining measurements, and ability in object tracking, both systems are equipped with the same hardware: optical tube, telescope mount, and sCMOS sensor. The sensors were chosen for both the high quantum efficiency and the high frame rate achievable, which allows to obtain a huge number of measurements in a brief time interval; the mounts because of their capability to follow all objects in all orbital regime. The synchronization is given by a GPS sensor assembled in both systems.

Figure 2. Fast Imaging and Tracking System (FITS): are shown respectively on the left SCUDO observatory, located in Collepardo (FR), and on the right RESDOS observatory, located on Rome (RM)

A summary of the main characteristics of the system are reported in Tab. 1.

Table 1. Main characteristics of FITS observatory system

Sensor type	sCMOS
Sensor diagonal	22 mm
Max fps	100
Diameter	150 mm
Mount type	Equatorial

3 SYNCHRONIZATION TESTS

To perform a multi-site observation, it is necessary to have a system able to collect simultaneously data of the same object, i.e., the systems must be synchronized. The higher the synchronization error the higher the error on the estimate of the altitude of the object. In this framework, several tests were conducted in order to minimize this kind of error. The sources of error in this sort of systems can be due to the Pulse Per Second (PPS) signal of the GPS, incompatibility of the frame rate of the cameras. The PPS of the GPS signal error is on average 20 ns, for signal construction [13], but it was also controlled with the oscilloscope seeing the time difference between two signals received from the GPS modules. This error is negligible.

The frame rate consistency and the synchronization between the cameras were checked using a chronometer built at CoBBS Lab and specifically designed for these tests: a needle spins at a constant rotational velocity (1rps) over a protractor, therefore the needle spans an angle of 1 degree in 3ms. Therefore, the chronometer can be used as a clock and the time can be measured from the angle span by the needle. The frame rate consistency was tested for each camera separately, by measuring the angle span by the needle between two subsequent images. A negligible error was found, i.e., the error is below the resolution of 3ms (corresponding to 1deg at a rotational speed of 1rps). Moreover, the synchronization between the cameras was tested, comparing the position of the needle on the images acquired at the same time frame from different cameras and once again a negligible error occurred.

4 MEASURES CALIBRATION

In order to achieve results as precise as possible, FITS is calibrated in terms of time. The measures calibration routine takes as input the data obtained through the optical observations and the Precise Orbit Ephemeris (POE) released by the satellites' owner. The POE could be provided in different format: Earth Orientation File (EOF), Consolidate Prediction File (CPF) and Standard Product 3 (SP3). Since not all the satellites released the POE, a research was conducted for the ones those who provide the ephemeris file. This research led the team to choose the Earth observation satellites Sentinel 1 A (NORAD ID 39634, Int. Design. 2014-016A).

The ESA's Copernicus project team releases, every 20 days from the current day, the Sentinel ephemeris in EOF format. Initially, the calibration routine makes an analysis of the measures without considering time correction and computing the residual mean and the covariance eigenvalues by just comparing the observations data and the ephemeris. Therefore, a time analysis can be performed in order to understand how much the obtained measures differ from the ones

obtained from ephemeris in terms of time. Since the POE of the Sentinel are released every 10 seconds, an interpolation procedure between two known consecutive ephemeris data is applied for the time of the measures that fall into this interval. The output of this procedure is the time bias, i.e., how much the time shift should be to reduce the residual mean. In particular, during the time bias analysis, an optimization routine of a cost function expressed in terms of residual mean occurs. In this way the measures obtained from optical observations can be corrected in time. The Fig. 3 and 4 show the results of the calibration routine conducted on measures obtained from Sentinel 1A observation on December 16th, 2020 and the Tab. 2 propose the results of the calibration routine in number.

Table 2. Residual mean both with time bias analysis and without it

Res. mean	RESDOS		SCUDO	
	RA [deg]	Dec [deg]	RA [deg]	Dec [deg]
No time analysis	0.0188	-0.0145	0.0386	-0.0388
With time analysis	0.0034	0.0032	0.0023	0.0021
Time bias	0.056 s		0.135 s	

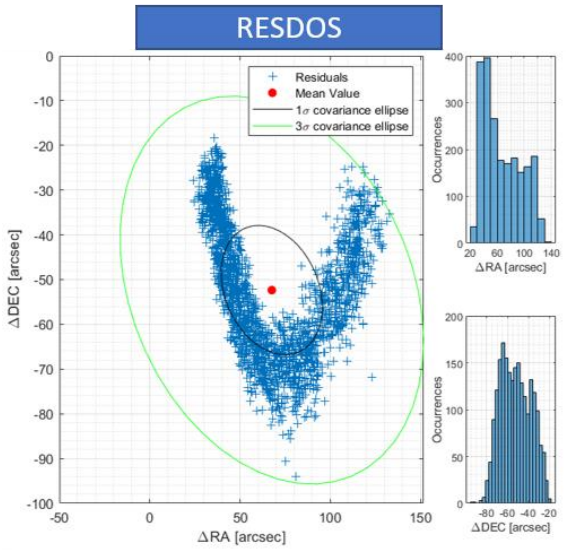

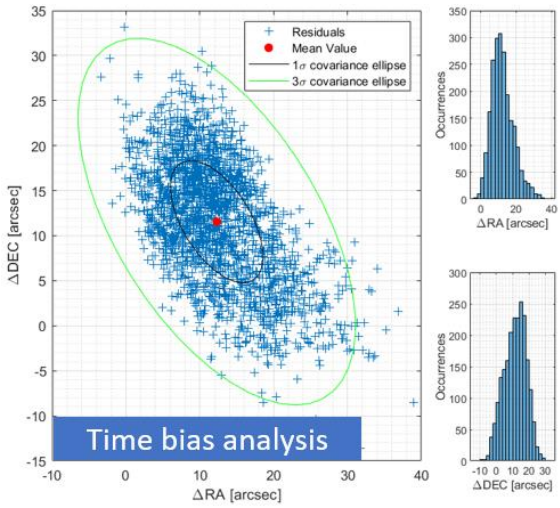

Figure 3. Residual means related to the measures acquired from RESDOS without time bias analysis (left) and with time bias analysis (above)

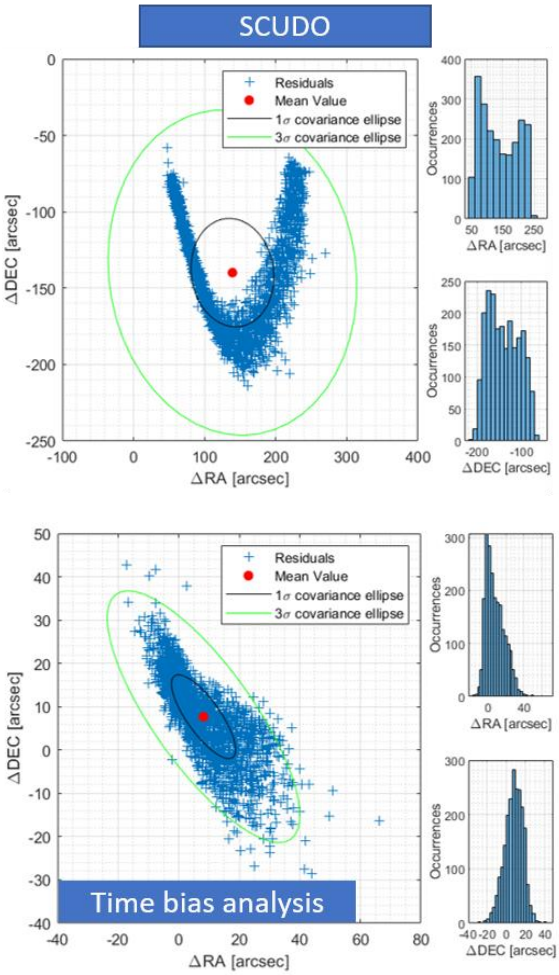

Figure 4. Residual means related to the measures acquired from SCUDO without time bias analysis (above) and with time bias analysis (bottom)

The time bias analysis demonstrates the good timing of the two observation systems. Fig. 5 shows the simultaneous light-curve of the Sentinel 1A during the passage use for the time bias analysis. It is possible to notice a peak due to the high reflectivity of the body.

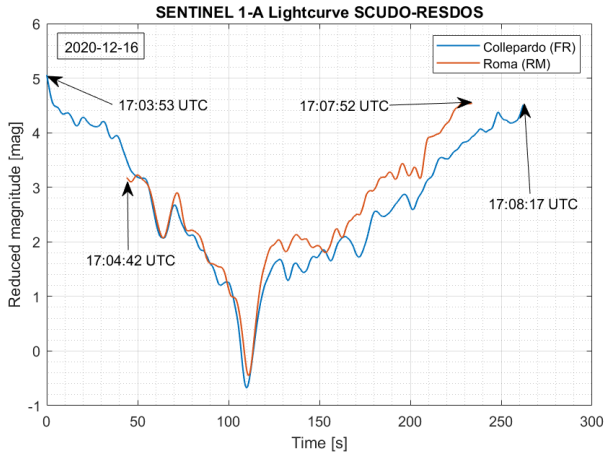

Figure 5. Sentinel 1A bi-static light-curve obtained with FITS system during the passage of 2020/12/16 from 17:03:53 to 17:08:17 UTC

5 OPTICAL LIGHT-CURVE

The light-curve of an object is defined as the variation over time of its apparent magnitude. By definition, the apparent magnitude of a body is computed with respect to the magnitude of another one, therefore a comparison object is needed. For an orbiting object, the stars present in the field of view are chosen as reference. In this way the retrieved magnitude of the object is clear from the possible presence of cloud or misty. Therefore, a star field resolution is necessary. This procedure is carried out performing a local version of the Astrometry.net [14] and using the Tycho-2 star catalogue. The catalogue contains position, proper motions, and photometric data for the 2.5 million brightest stars in the sky vault [15]. From the star field resolution is therefore possible to obtain the position of the stars, both in terms of celestial coordinates (right ascension and declination) and pixel coordinates, bolometric and visual magnitude. All these parameters are used in the analysis after the image acquisition

5.1 Light-curve acquisition procedure

Once the images of the passage above the observatory are obtained, the procedure to retrieve the real light-curve of the object from both optical systems can occur. In order to analyze the thousands of frames that compose the video, an automatic software was developed by the S5Lab research team. The software takes in input all frames, and for each of them performs a photometric calculation in order to find the stars present in FoV that will be used as reference in the object magnitude computation and therefore in the light-curve reconstruction. Given that the light is reduced with the distance the light-curve is normalized with respect to the range. In Fig. 6 the flowchart of the software is proposed.

For calculation of the star and object intensity (I) the aperture photometry procedure is performed [16]. The total integrated photometric source signal (S) is computed as the sum of the pixels contained in the area (A) defined as the circle that surround the star or object. Moreover, a background estimation (B) is evaluated, considering a circular crown in the neighborhood of the star/object and centered on it, see Fig. 5. Once S and B are retrieved, is possible to compute the intensity using the Eq. 1:

$$I = S - n_{pix} \cdot B \tag{1}$$

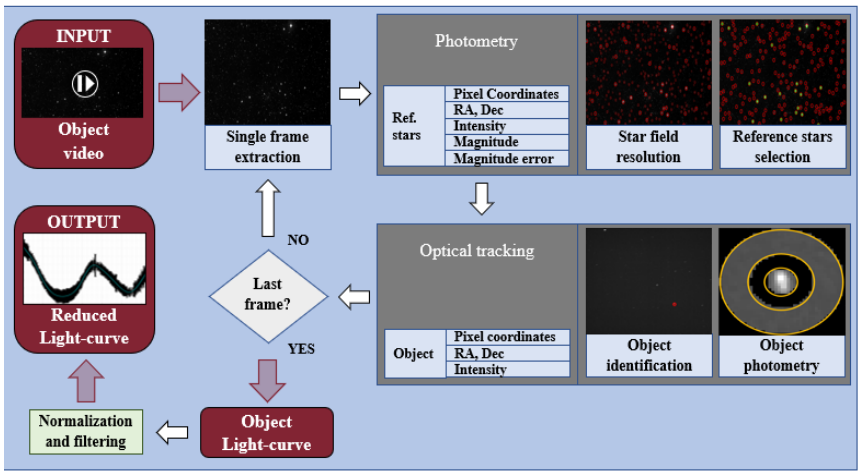

Figure 6. High-level flow-chart of the software for video analysis

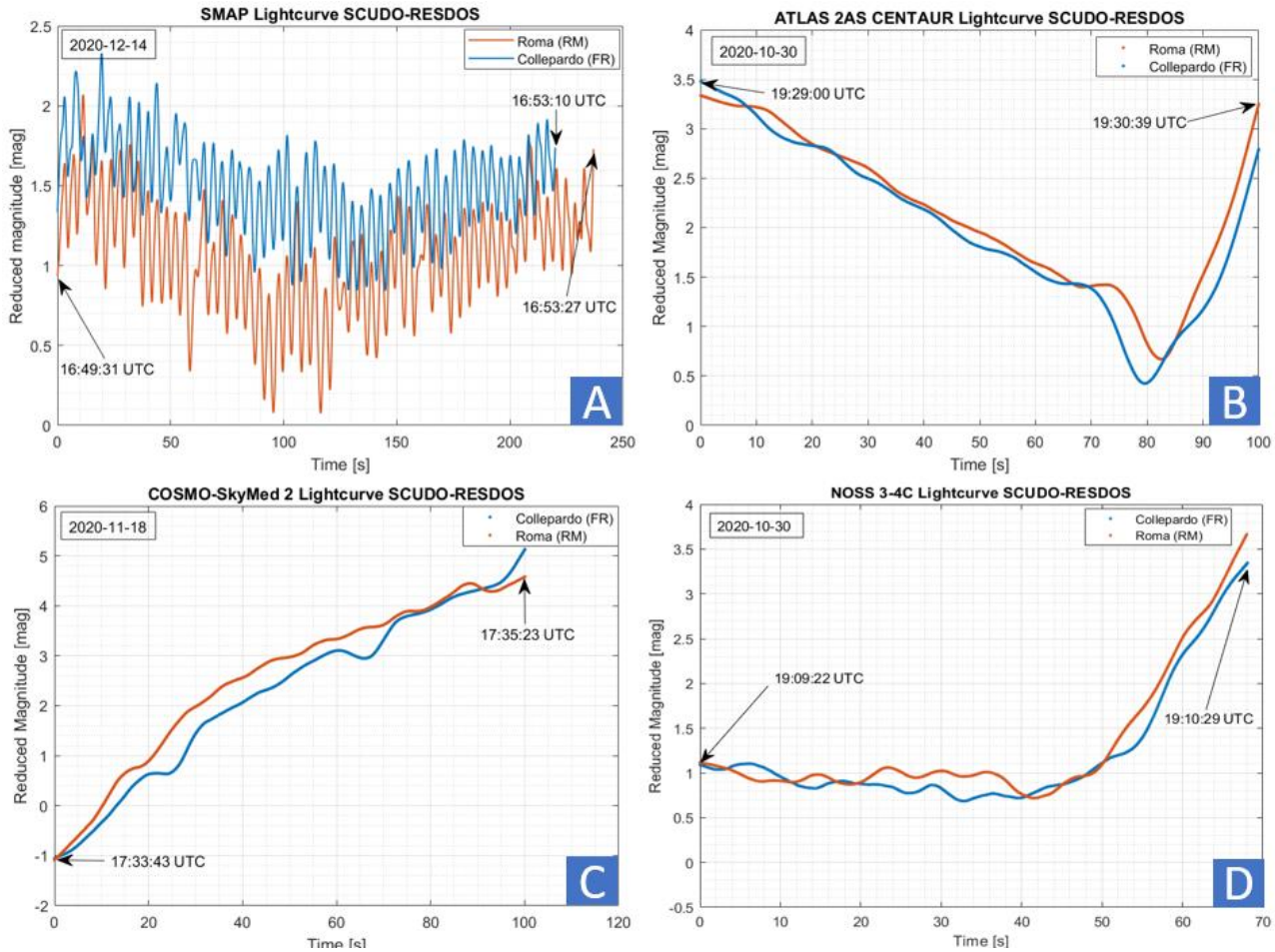

Figure 7. (A) SMAP bi-static light-curve obtained with FITS system during the passage of 2020/12/14 from 16:49:30 to 16:53:27 UTC, (B) ATLAS 2AS CENTAUR R/B bi-static light-curve obtained with FITS system during the passage of 2020/10/30 from 19:29:00 to 19:30:39 UTC, (C) Cosmo-SkyMed 2 bi-static light-curve obtained with FITS system during the passage of 2020/11/18 from 17:33:43 to 17:53:23 UTC, (D) NOSS 3-4C R/B bi-static light-curve obtained with FITS system during the passage of 2020/10/30 from 19:09:22 to 19:10:29 UTC

where n_{pix} is the total number of pixels contained within the area A and B is the background. It can be seen that the intensity value of the object depends on the radius of the circle that is used to outline it. In [17, 18] is shown how the signal to noise ratio (SNR) of an object is maximized for a particular value of this radius. Maximizing the SNR means to minimize the error in the intensity calculation.

Once the intensity of the object and stars are computed, the apparent magnitude of the object can be calculated using the catalogue magnitude of the stars in the Field of View (FoV), as shown in Eq. 2.

$$mag_{obj} = mag_{star_{j,cat}} - 2.5log\left(\frac{I_{obj}}{I_{star_j}}\right) \quad (2)$$

where mag_{obj} is the object's magnitude, I_{obj} is its intensity, $mag_{star,jcat}$ is the catalogue magnitude of the j-th star and $I_{star,j}$ is its intensity. The object's magnitude is then calculated with respect to all the stars in the FoV. Therefore, it is possible to compute the apparent magnitude of the object as the mean of those previously calculated plus or minus the standard deviation of the measurements. Furthermore, it is possible to select only one sub-group of stars present in the FoV, in order to minimize the standard deviation of the magnitude error.

5.2 Simultaneous light-curve

Once the analysis of the video is completed, it is possible to retrieve the light-curve of the object. The FITS system, as previously mentioned, allows to obtain the light-curve of the same object at the same time. Fig. 7A give an example of the simultaneously light-curves obtained during a bi-static observation taken from RESDOS and SCUDO observatories. The figure shows the results of the observation of the Earth observation satellite Soil Moisture Active Passive (SMAP) during its passage of December 14th, 2020 from 16:49:30 to 16:53:27 UTC. The error is not represented for visualization purposes. The red curve is the light-curve obtained from RESDOS observatory, while the blue one

from SCUDO observatories.

In order to validate the outputs of the software for the light-curve reconstruction, several observations for different objects were conducted from October to January 2021. The observed bodies were both operative satellites and space debris. In this framework, the research team takes part to the IADC campaign WG1 AI 38.2 "Attitude motion characterization of LEO upper stages using different observation techniques". In Tab. 2 are shown the total number of observations, including the IADC objects and the simultaneous results are specified.

Table 3. Total observations between October 2020 and January 2021, both for space debris (SD) and operative satellites (OS), recorded by FITS.

Total observations			
Observed objects	41	**SD**	18
		OS	23
Light-curves	95	**RESDOS**	36
		SCUDO	59
Simultaneous light-curves		20	

In Fig. 7B, 7C, and 7D other examples of simultaneous light-curve are shown.

The differences between the light-curves retrieved by the two observatories (red and blue curves) are due to the different point of view from which the satellites is observed. These variations are useful for the attitude reconstruction of the observed object [19].

6 CONCLUSION

In this work first results of simultaneous observation of LEO objects was presented. To this aim, the S5Lab team together with the one of the ICS used a bistatic observation strategy exploited by the FITS optical system. To check the synchronization of the whole system, several laboratory tests was conducted in order to minimize the timing errors. Moreover, a time bias analysis is performed using the Sentinel 1A POE data released by the ESA's Copernicus project. This analysis allows to check the timing difference between the obtained measures and the ephemeris one. The analysis of the obtained optical data is performed automatically through a software which uses photometric computation in order to retrieve the magnitude variation over time (light-curve) of the object. The results obtained with the proposed methods are very promising for a future development in the altitude and attitude reconstruction purpose.

7 ACKNOWLEDGMENT

This work is supported by the Italian Research Project MODDS (Monitoraggio Detriti Spaziali Stereo) ID 85-2017-14966, "Progetto di Gruppo di Ricerca finanziato ai sensi della L.R. Lazio 13/08".

8 REFERENCES

1. ESA Space Debris Office, *ESA's Annual Space Environment Report*, GEN-DB-LOG-00288-OPS-SD
2. ESA, Space Debris by the Numbers, European Space Agency. Available online: https://www.esa.int/Our_Activities/Operations/Space_Debris/Space_debris_by_the_numbers (accessed on 28 June 2018).
3. NSTCC. The National Science and Technology Council Committee on Transportation Research & Development; Interagency Report on Orbital Debris 1995; NSTCC: Washington, DC, USA, 1995.
4. Adushkin, V.V. & Aksenov, O.Yu & Veniaminov, S.S. & Kozlov, Stanislav & Tyurenkova, Veronika. (2020). The Small Orbital Debris Population and its Impact on Space Activities and Ecological Safety. Acta Astronautica. 176. 10.1016/j.actaastro.2020.01.015.
5. Acernese, M. et al. Improving accuracy of LEO objects Two-line elements through optical measurements. In Proceedings of the 69th International Astronautical Congress, Bremen, Germany, 1–5 October 2018. IAC-18,A6,9,8,x47421.
6. Piergentili, F., Santoni, F., Seitzer, P., Attitude Determination of Orbiting Objects from Lightcurve Measurements, (2017) IEEE Transactions on Aerospace and Electronic Systems, 53 (1), art. no. 7819454, pp. 81-90
7. Porfilio, M., Piergentili, F., Graziani, F., The 2002 Italian optical observations of the geosynchronous region, (2003) Advances in the Astronautical Sciences, 114 II, pp. 1237-1252.
8. Pastore, R., Delfini, A., Micheli, D., Vricella, A., Marchetti, M., Santoni, F., Piergentili, F., Carbon foam electromagnetic mm-wave absorption in reverberation chamber, (2019) Carbon, 144, pp. 63-71.
9. Piattoni, J., Ceruti, A., Piergentili, F., Automated image analysis for space debris identification and astrometric measurements, (2014) Acta Astronautica, 103, pp. 176-184.
10. Micheli, D., Santoni, F., Giusti, A., Delfini, A., Pastore, R., Vricella, A., Albano, M., Arena, L., Piergentili, F., Marchetti, M., Electromagnetic absorption properties of spacecraft and space debris, (2017) Acta Astronautica, 133, pp. 128-135.
11. Piergentili, F., Porfilio, M., Graziani, F., Optical campaign for low earth orbit satellites orbit determination, (2005) European Space Agency, (Special Publication) ESA SP, (587), pp. 689-692.

12. Shariar Hadji Hossein, Marco Acernese, Tommaso Cardona, Giammarco Cialone, Federico Curianò, Lorenzo Mariani, Veronica Marini, Paolo Marzioli, Leonardo Parisi, Fabrizio Piergentili, Fabio Santoni; Sapienza Space debris Observatory Network (SSON): A high coverage infrastructure for space debris monitoring. Journal of Space Safety Engineering, Volume 7, Issue 1, March 2020, Pages 30-37.

13. M. Siccardi, About time measurements, EFTF 2012.

14. Hogg, D.W.; Blanton, M.; Lang, D.; Mierle, K.; Roweis, S. Automated Astrometry, Astronomical Data Analysis Software and Systems XVII. Available online:http://adsabs.harvard.edu/full/2008ASPC.394..27H (accessed on 12 December 2020).

15. Høg, E.; Fabricius, C.; Makarov, V.V.; Urban, S.; Corbin, T.; Wycoff, G.; Bastian, U.; Schwekendiek, P.; Wicenec, A. The Tycho-2 Catalogue of the 2.5 Million Brightest Stars; Naval Observatory: Washington, DC, USA, 2000.

16. Howell, S. Handbook of CCD Astronomy, 2nd ed.; Cambridge University Press: Cambridge, UK, 2006.

17. Howell, S.B. Two-dimensional aperture photometry-Signal-to-noise ratio of point-source observations and optimal data-extraction techniques. Publ. Astron. Soc. Pac. 1989, 101, 616.

18. Stetson, P.B. On the growth-curve method for calibrating stellar photometry with CCDs. Publ. Astron. Soc. Pac. 1990, 102, 932.

19. Fabrizio Piergentili, Gaetano Zarcone, Leonardo Parisi, Lorenzo Mariani, Shariar Hadji Hossein and Fabio Santoni, LEO Object's Light-Curve Acquisition System and Their Inversion for Attitude Reconstruction, Aerospace 2021, 8(1), 4; doi:10.3390/aerospace8010004